Crossover Formation During Rice Meiosis Relies on Interaction of OsMSH4 and OsMSH5

Lei Zhang,*,[1] Ding Tang,*,[1] Qiong Luo,[†] Xiaojun Chen,*,[‡] Hongjun Wang,* Yafei Li,* and Zhukuan Cheng*,[2]
*State Key Laboratory of Plant Genomics and Center for Plant Gene Research, Institute of Genetics and Developmental Biology, Chinese Academy of Sciences, Beijing 100101, China, [†]Ministry of Education Key Laboratory of Agriculture Biodiversity for Plant Disease Management, Yunnan Agricultural University, Kunming 650201, China, and [‡]Ningxia Academy of Agriculture and Forestry Sciences Agricultural Biotechnology Center, Yinchuan 750002, China
ORCID ID: 0000-0001-8428-8010 (Z.C.)

ABSTRACT *MSH4* encodes a MutS protein that plays a specialized role in meiosis. In eukaryotic species, such as budding yeast, mice, *Caenorhabditis elegans*, and *Arabidopsis*, *msh4* mutants display meiotic defects with a reduced number of chiasmata. Here, we characterized rice *MSH4* by map-based cloning. In *Osmsh4* mutants, the chiasma frequency was dramatically decreased to ~10% of the wild type, but the synaptonemal complex was normally installed. The double mutant analysis showed that in the *Osmsh4 Osmsh5* mutant, the reduction of chiasmata was greater than other *zmm* mutants. This was consistent with the absence of localization for OsZIP4 and OsMER3 in *Osmsh4* and suggests an earlier role for OsMSH4 and OsMSH5 than other ZMM proteins where they may be required to stabilize progenitor Holliday junctions. Using yeast two-hybrid and pull-down assays, we verified the direct physical association between OsMSH4 and OsMSH5 and OsMSH5 and HEI10 in plants for the first time. The MSH4–MSH5 heterodimer has been demonstrated in mammals to stabilize the formation of progenitor and double Holliday junctions that may be resolved as crossovers (COs). We propose that OsMSH4 interacts with OsMSH5 to promote formation of the majority of COs in rice.

MEIOSIS is a special form of cell division that generates haploid gametes for sexual propagation. Meiocytes undergo an intricate and elaborate process: one round of chromosome replication is followed by two rounds of cell division, the unique meiosis I and the mitosis-like meiosis II, generating four haploid gametes. The first division segregates homologous chromosomes, whereas the second one splits sister chromosomes, thereby halving the chromosome content from diploid to haploid. The first division has been recognized as the crucial stage of meiosis, in which prophase I is particularly important. Prophase I can be divided into five dissimilar but inseparable stages according to their different chromosome structures and behaviors: leptotene, zygotene, pachytene, diplotene, and diakinesis, during which homologous chromosomes pair, synapse, and recombine (Zickler and Kleckner 1999; Li and Ma 2006).

doi: 10.1534/genetics.114.168732
Manuscript received July 23, 2014; accepted for publication September 29, 2014; published Early Online October 2, 2014.
Supporting information is available online at http://www.genetics.org/lookup/suppl/doi:10.1534/genetics.114.168732/-/DC1.
[1]These authors contributed equally to this work.
[2]Corresponding author: Institute of Genetics and Developmental Biology, Chinese Academy of Sciences, Beijing 100101, China. E-mail: zkcheng@genetics.ac.cn

Pairing, synapsis, and recombination are well linked in a carefully coordinated mechanism. Homologs search out and pair with each other, facilitating the initiation of recombination. Meanwhile, early stages of recombination are also used to promote global pairing and synapsis of homologs. Mature synaptonemal complexes (SCs) form as the homologous chromosomes approach each other at a distance of 100 nm and are disassembled during diplotene (Sym and Roeder 1994). After the disassembly of SCs, homolog pairs are held together only by crossovers (COs) to ensure their alignment on the metaphase I plate. COs also create physical connections between homologous chromosomes to guarantee their normal segregation to the opposite poles. In consequence, the absence of COs causes random segregation of homologs at anaphase I, leading to the formation of aneuploid dyads and a reduction of bivalents, followed by the segregation of sister chromosomes in anaphase II to produce aneuploid tetrads at the end of meiosis (Ross-Macdonald and Roeder 1994; de Vries *et al.* 1999; Lipkin *et al.* 2002; Chen *et al.* 2005). COs are believed to correspond to homologous recombination sites, visualized as chiasmata under the microscope.

Homologous recombination begins with DNA double-strand breaks (DSBs) catalyzed by SPO11 protein (Keeney *et al.* 1997). DSBs are further processed by MRX complex

(Mre11–Rad50–Xrs2) and two DNA strand-exchange proteins DMC1/RAD51 to initiate the strand exchange and produce double Holliday junctions (dHjs) (Baumann *et al.* 1996; Li *et al.* 1997; Schwacha and Kleckner 1997; Puizina *et al.* 2004; Osman *et al.* 2011). Reciprocal exchanges between homologous chromosomes occur to generate COs or noncrossovers (NCOs) (Allers and Lichten 2001; Borner *et al.* 2004; Lynn *et al.* 2007).

The ZMM proteins (Zip1–4, Mer3, Msh4, Msh5, and Spo16), initially characterized in *Saccharomyces cerevisiae* and found conserved in almost all eukaryotes, have been shown to play critical roles in processing of a subset of recombination interactions at sites destined to become COs (Borner *et al.* 2004; Lynn *et al.* 2007; Youds and Boulton 2011). Accordingly, elimination of the majority of COs was detected in *zmm* mutants of many species, including budding yeast (Ross-Macdonald and Roeder 1994; Tsubouchi *et al.* 2006), mammals (Mercier *et al.* 2001; Nakagawa *et al.* 2001; Novak *et al.* 2001; Neyton *et al.* 2004), and plants (Higgins *et al.* 2004; Wang *et al.* 2009; Shen *et al.* 2012).

MutS family proteins together with MutH and MutL function in repair of DNA mismatches in bacteria. In eukaryotic species, there are six MutS proteins (Msh1–6). Among them, Msh2, Msh3, and Msh6 have been shown to take part in DNA mismatch repair (MMR) (Borts *et al.* 2000; Kolas and Cohen 2004), whereas only Msh4 and Msh5 are revealed to specifically get involved in the meiotic recombination process but not in MMR (Ross-Macdonald and Roeder 1994; Hollingsworth *et al.* 1995; Zalevsky *et al.* 1999; Kneitz *et al.* 2000; Novak *et al.* 2001; Higgins *et al.* 2004; Hoffmann and Borts 2004; Kolas and Cohen 2004; Neyton *et al.* 2004; Her *et al.* 2007). In *S. cerevisiae*, mutations in *Msh4* and *Msh5* lead to the disruption of CO formation and the nondisjunction of homologous chromosomes (Ross-Macdonald and Roeder 1994; Hollingsworth *et al.* 1995). In *Caenorhabditis elegans*, MSH4 plays a decisive role in CO formation, as research has shown that the mutation in *him-14*, the ortholog of budding yeast *Msh4*, completely eliminates the COs (Zalevsky *et al.* 1999). In mouse strains lacking MSH4 or MSH5, COs are entirely eliminated and homologous chromosomes fail to align properly, resulting in both male and female sterility (de Vries *et al.* 1999; Edelmann *et al.* 1999; Kneitz *et al.* 2000). In *Arabidopsis*, chiasma frequency is greatly reduced in *Atmsh4* and *Atmsh5* in comparison to the wild type (Higgins *et al.* 2004, 2008). MSH4 and MSH5 can form a heterodimer (Bocher *et al.* 1999; Snowden *et al.* 2004), which binds to single Holliday junctions or three-armed progenitor Holliday junctions as a sliding clamp embracing the homologous chromosomes and promoting the formation of COs (Borner *et al.* 2004; Snowden *et al.* 2004).

Rice is a popular plant model for molecular biological studies and one of the world's most important food crops. With the complete sequencing of the rice genome, there have been great achievements in functional genomic studies. Using genetic analysis combined with cytology, many genes related to rice meiosis have been discovered and their functions further characterized (Luo *et al.* 2014). In this study, we identified the rice homolog of MSH4 by map-based cloning, investigated its function in CO formation, and demonstrated its relationship with other ZMM proteins. Our genetic and cytological data suggested that the loss of *OsMSH4* function resulted in a more severe diminution in CO formation than other *zmm* mutants. We also validated that OsMSH4 in combination with OsMSH5 might promote formation of the majority of crossover. In addition, we demonstrated an interaction between OsMSH5 and HEI10, providing further evidence for the intimate relationships among ZMM proteins.

Table 1 Chiasma frequency in different genotypes

Genotype	Chiasma/cell	Reference
Wild type	20.56 ± 1.49 (n = 47)[a]	This study
Osmsh4-1	1.71 ± 1.25 (n = 204)	This study
Osmsh5-1	2.10 ± 0.91 (n = 97)	Luo *et al.* (2013)
Oszip4	6.05 ± 1.97 (n = 164)	Shen *et al.* (2012)
Osmer3	5.59 ± 2.07 (n = 64)	Shen *et al.* (2012)
hei10	6.50 ± 2.10 (n = 130)	Wang *et al.* (2012)
Osmsh4 Osmsh5	1.76 ± 1.20 (n = 115)	This study

[a] Mean ± SD n, number of pollen mother cells observed.

Materials and Methods

Plant materials

Osmsh4-1 and *Osmsh4-4* were identified from an *indica* rice variety, Zhongxian 3037, induced by ^{60}Co-γ ray radiation. *Osmsh4-2* and *Osmsh4-3* were *TOS17* insertion lines provided by the Rice Genome Resource Center of the National Institute of Agrobiological Sciences (https://tos.nias.affrc.go.jp/). The *Osmsh5* allele employed in this study is *Osmsh5-1* (Luo *et al.* 2013). Zhongxian 3037 was used as the wild type in the related experiments. Paddy fields were applied to cultivate rice materials required for both gene mapping and functional characterization.

Molecular cloning of OsMSH4

STS markers were designed based on the sequence differences between the *indica* rice variety 9311 and the *japonica* rice variety Nipponbare on the basis of data published on the National Center for Biotechnology Information website (http://www.ncbi.nlm.nih.gov) (Supporting Information, Table S1).

The reverse transcription was performed as previously described (Shen *et al.* 2012). The BD SMART RACE cDNA Amplification kit (Clontech) was used to perform the following amplification according to the manufacturer's instructions. Two gene-specific primers, 5RACER1 (5′-CTGATAAATGTTGCGAAG-3′) and 5RACER2 (5′-CTAGTTGAGTCAATGTTCA-3′) were combined with the general adaptor primers supplied by the kit. For 3′-RACE, two rounds of PCR were performed with the same 3′-adaptor primer (5′-CTGATCTAGAGGTACCGGATCC-3′) and two *OsMSH4* gene-specific primers, 3RACEF1 (5′-GTTGCT CGTAGATCTTTCTGT-3′) and 3RACEF2 (5′-ACTTCACGGATCA CAGAACA-3′). The products of 3′-RACE-PCR and 5′-RACE-PCR were cloned and sequenced.

Construction of RNAi cassette and rice transformation

A 380-bp fragment was amplified and cloned into pMD18T vector (Takara). A single clone, proven by sequencing to be an accurate copy with no mutations, was used to generate a 380-bp fragment and further cloned into the *Bgl*II/*Xho*I and *Bam*HI/*Sal*I sites of the pUCRNAi vector. The resulting stem-loop fragment was then cloned into the binary vector pCAMBIA2300-actin. Finally, the RNAi construct was transformed into *Agrobacterium tumefacien* strains for further plant transformation.

Yeast two-hybrid assay

The yeast two-hybrid assays were conducted using the Matchmaker Gold Yeast Two-Hybrid system with ZMM proteins, including OsMSH4, OsMSH5, and HEI10. ORFs of the related genes were amplified using the 2× Power Taq PCR Mastermix I (BioTeKe) and cloned into pGADT7 and pGBKT7 to generate AD and BD recombinants. Those plasmids were cotransformed into Y2H Gold strain in an AD–BD-coupled manner.

α-Galactosidase activity was qualitatively monitored using the blue color reporter assay on quadruple dropout (QDO) selection medium with aureobasidin A and the chromagenic substrate X-α-Gal (SD −Leu −Trp −Ade −His +aureobasidin A +X-α-Gal). Positive clones turned blue in the presence of X-α-Gal, while negative clones were even unable to grow. The yeast strains transformed with both vectors were also plated on double dropout (DDO) selecting medium (SD −Leu −Trp) to confirm the successful transformation.

Pull-down assay

OsMSH4 and HEI10 coding sequences were separately cloned into pMAL-c5x (NEB), while the OsMSH5 coding sequence was cloned into pGEX4T-2 (Amersham). All these recombinant vectors and empty vectors were transformed into *Escherichia coli BL21* (DE3) individually and 0.2 mM isopropyl β-D-thiogalactoside (IPTG) was added to induce the expression of those proteins. The cell lysate containing 25–50 mg GST-fused OsMSH5 or GST tag were incubated with 200 μl 50% glutathione sepharose 4B beads (GE Healthcare) at 4° for 2 hr under gentle agitation. After that, the coated GST-fused protein beads were washed three times in 1× phosphate-buffer saline (PBS) solution. Then the cell lysates containing 25–50 mg MBP-fused proteins or MBP tag were added into the washed GST-fused protein beads. After 1 hr of incubation at 4° under gentle agitation, the bound protein–bead complexes were sedimented by centrifugation and washed five times in 1× PBS solution. Then, the beads were resuspended in 50 μl SDS-PAGE loading buffer and heated for 10 min in the boiled water. Protein samples were resolved on 10% SDS-PAGE gels for further blotting analysis using an anti-MBP antibody.

Meiotic chromosome preparation

Young panicles from both wild-type and *Osmsh4* plants were collected and fixed in Carnoy's solution (ethanol:glacial acetic = 3:1). Anthers at meiotic stages were quickly squashed in an acetocarmine solution onto glass slides and then frozen in liquid nitrogen. After lifting and removing coverslips, slides were dehydrated using an ethanol gradient (70, 90, and 100%). Chromosome spreads were counterstained with 4′,6-diamidino-2-phenylindole (DAPI) in an antifade solution (Vector Laboratories, Burlingame, CA). Images were captured under a Zeiss A2 fluorescence microscope with a micro-charge-coupled device camera.

Immunofluorescence

Fresh young panicles were fixed in 4% (w/v) paraformaldehyde for 30 min at room temperature. Anthers in the meiotic stage were squashed with a dissecting needle in 1× PBS solution and covered with a coverslip. After prying up coverslips, slides were dehydrated using an ethanol gradient (70, 90, and 100%). Slides harboring anthers were incubated in a humid chamber at 37° for ∼4 hr with different combinations of antibodies, all diluted 1:500 in TNB buffer (0.1 M Tris-HCl, pH 7.5, 0.15 M NaCl, and 0.5% blocking reagent). After three rounds of washing in 1× PBS, Texas Red-conjugated goat antirabbit antibody and fluorescein isothiocyanate-conjugated sheep antimouse antibody (1:1000) were added to the slides.

Results

Isolation of a sterile mutant

We isolated a mutant from the self-fertilization line of an *indica* rice variety, Zhongxian 3037, induced by ^{60}Co-γ ray radiation. The mutant plant showed normal vegetative growth and development (Figure S1A), but was almost sterile (Figure S1B). Its pollen grains were empty and shrunken and could not be stained by I_2-KI (Figure S1, C and D). Furthermore, we checked the viability of female gametes by pollinating its flowers with the wild-type pollens. There was no seed produced, indicating that the female gametes were also affected by this mutation.

We also verified that the sterile phenotype of *Osmsh4-1* was controlled by a single recessive gene, via calculating the segregation ratio of the progeny delivered from a self-fertilized heterozygous plant. There were 73 fertile plants and 25 sterile plants, which is consistent with a 3:1 segregation ($\chi^2 = 0.22$, $P > 0.05$).

Identification of the OsMSH4 gene

To identify the gene responsible for the sterile phenotype, a large F_2 mapping population was constructed by crossing the heterozygous plants with a *japonica* rice variety Zhonghua11. The F_2 and F_3 sterile segregates, amounting to 732 individual plants in total, were collected for further map-based cloning. The gene was initially mapped to the long arm of chromosome 7 and finally confined to a 110-kb region.

Within this region, a candidate gene (Os07g0486000) was identified and the protein was depicted as a MutS family protein resembling MSH4 in other organisms such as *Arabidopsis* (75% identity/87% positive), *Brachypodium distachyo* (91% identity/95% positive), mouse (35% identity/58%

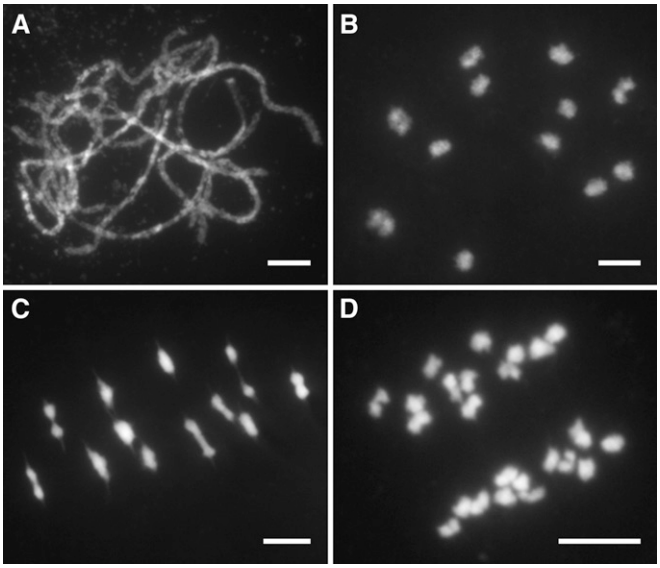

Figure 1 Meiotic chromosome behaviors of PMCs in the wild type. (A) Pachytene. (B) Diakinesis. (C) Metaphase I. (D) Anaphase I. Chromosomes were stained with DAPI. Bars, 5 μm.

positive), and *S. cerevisiae* (29% identity/50% positive). In addition, this mutant was found to have similar defects with *msh4* mutants in other species, including reduced fertility on a macroscopic scale and desynapsis on a microscopic scale, which increased the likelihood that *OsMSH4* was the candidate gene. We therefore amplified and sequenced the candidate gene. A point mutation, the transition of G to A, was detected in the seventh exon, creating a new stop codon and causing premature termination of protein translation.

To confirm the mutant phenotypes were caused by the loss of function of *OsMSH4*, an RNA interference transformation vector was constructed and transformed into the wild-type rice to silence its expression. From the transgenic plants, sterile plants were selected for further analysis. RT-PCR analysis demonstrated that the expression of *OsMSH4* in the sterile RNAi plants was markedly reduced compared to the wild type (Figure S3). Moreover, chromosome behavior in the meiocytes of sterile plants resembled that in the *Osmsh4* mutants (Figure S4D). We therefore drew the conclusion that the knockdown of *OsMSH4* led to the sterile phenotype.

In addition, three more *Osmsh4* mutants were identified (Figure S2A). Two of them are *Tos17*-insertion mutants provided by the Rice Genome Resource Center of the National Institute of Agrobiological Sciences; the other one was identified using the same mapping strategy with *Osmsh4-1* and this allele had a T-to-C mutation in the splicing site of intron 18. As *Osmsh4-1* is a deletion line creating a new stop codon, we selected it for further cytological investigation.

Characterization of the OsMSH4 gene

We performed 5′-RACE and 3′-RACE to find the 5′-UTR and 3′-UTR of *OsMSH4*, respectively. Meanwhile, primers were designed in the 5′-UTR and 3′-UTR to amplify the open reading frame (ORF). The full length of *OsMSH4* cDNA is

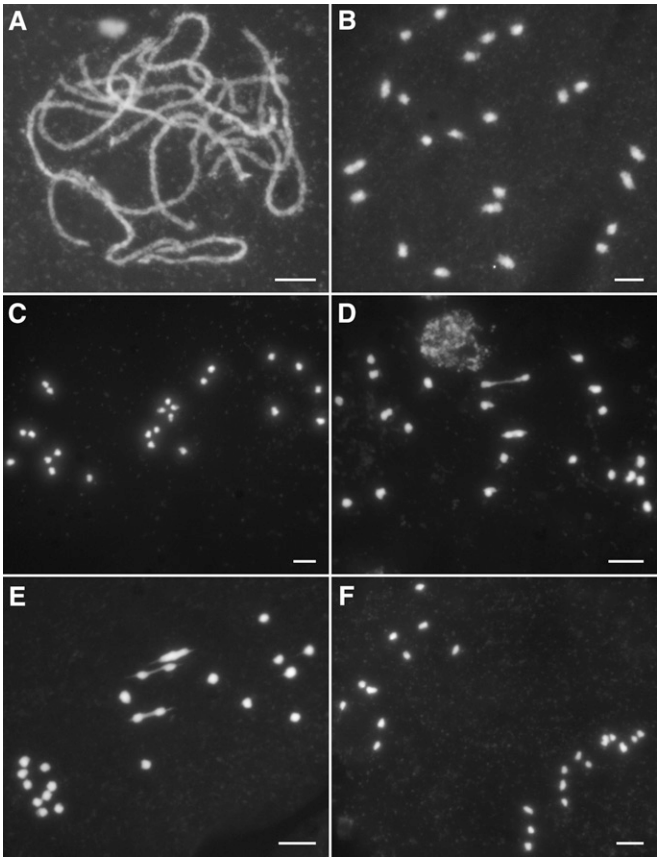

Figure 2 Meiotic chromosomes in *Osmsh4-1* meiocytes. (A) Pachytene. (B) Diakinesis. (C) Metaphase I with no bivalents. (D) Metaphase I with two bivalents. (E) Metaphase I with three bivalents. (F) Anaphase I. Bars, 5 μm.

2853 bp with an ORF of 2397 bp, which gives rise to 798 amino acids. The whole length of this gene is 9995 bp, comprising 24 exons and 23 introns (Figure S2A). OsMSH4 not only displays notable homology with MSH4 in *Arabidopsis* but also shows a close relationship to MSH4 in mammals and budding yeast (Figure S2B).

The expression patterns of *OsMSH4* in different organs were determined by RT-PCR analysis. *OsMSH4* transcripts were distributed among all organs; however, the expression in panicles was much higher than in other organs (Figure S3). In addition, the expression of *OsMSH4* was shown to be dramatically reduced in both *Osmsh4-1* and *OsMSH4*^{RNAi} plants (Figure S3).

Meiotic defects occur in Osmsh4 mutants

DAPI-stained meiotic chromosomes of pollen mother cells (PMCs) at different stages were investigated in both wild type and *Osmsh4-1*. In wild type, meiotic chromosomes were first seen as thin and tangled threads at leptotene and started to pair and synapse at zygotene. At pachytene, SCs were well established between homologous chromosomes (Figure 1A). Paired chromosomes were condensed into small dots and 12 rod-like or ring-like bivalents were distinctly visible at diakinesis (Figure 1B). All the bivalents lined up on the equatorial plate at

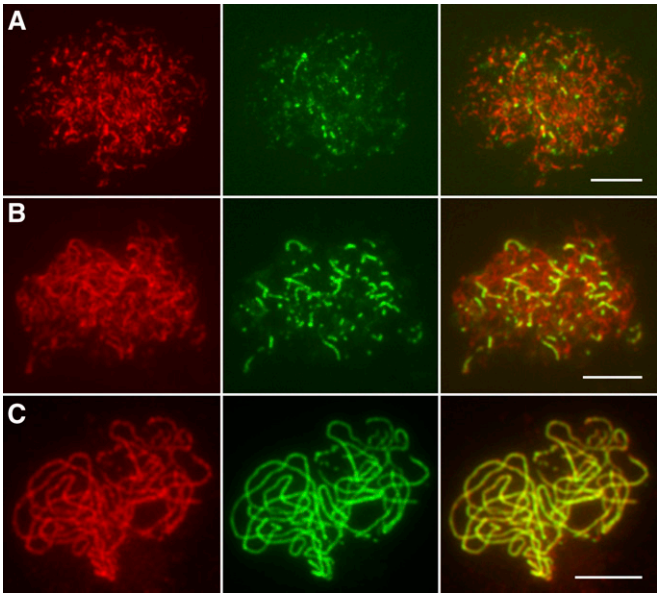

Figure 3 Immunolocalization of OsREC8 and ZEP1 in *Osmsh4-1*. (A) The localization of ZEP1 at leptotene. (B) The localization of ZEP1 at zygotene. (C) The localization of ZEP1 at pachytene. OsREC8 signals (red) were used to indicate chromosomes. Bars, 5 μm.

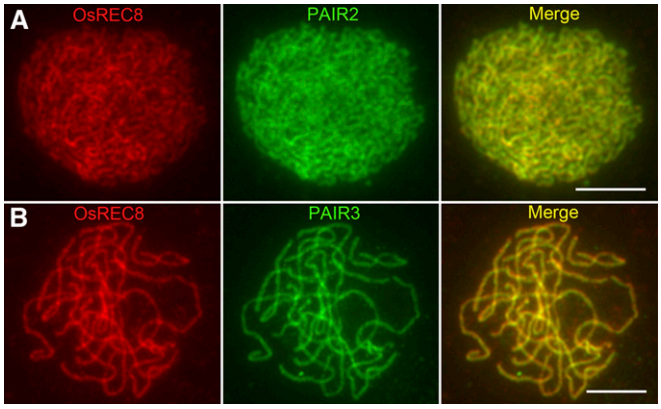

Figure 4 Immunolocalization of OsREC8, PAIR2, and PAIR3 in *Osmsh4-1*. (A) The localization of PAIR2 at zygotene. (B) The localization of PAIR3 at pachytene. OsREC8 signals were used to indicate chromosomes. Bars, 5 μm.

metaphase I (Figure 1C), followed by the separation of homologous chromosomes at anaphase I, which then migrated into two opposite poles (Figure 1D). The second meiotic division resembled mitosis, and during this process, sister chromatids of each chromosome separated from each other, generating four sets of 12 chromosomes in a tetrad at the end of meiosis.

Cytological investigation on the DAPI-stained meiotic chromosomes revealed a defective meiosis in *Osmsh4-1* meiocytes. From leptotene to pachytene, all the homologous chromosomes paired and synapsed (Figure 2A), showing the same chromosomes behave as the wild type. However, divergences from the wild type became apparent at diakinesis with the occurrence of many univalents (Figure 2B). At metaphase I, only 1.65 bivalents per PMC on average situated on the equatorial plate (n = 204), while the univalents dispersed within the whole nucleus (Figure 2, C–E). From anaphase I to telophase I, due to the random segregation of the univalents, chromosomes were separated unevenly into two daughter cells (Figure 2F). As a result, microspores with different numbers of chromosomes formed at the end of meiosis II. We also investigated chromosome behaviors in *Osmsh4-2*, *Osmsh4-3*, *Osmsh4-4*, and *OsMSH4*^{RNAi} plant meiocytes, which were very similar to those in *Osmsh4-1* (Figure S4, A–D).

The chiasma frequency is dramatically reduced in Osmsh4

We quantified the number of chiasmata both in *Osmsh4-1* and the wild type by evaluating the shape of bivalents at metaphase I, using the criteria described in a previous study (Sanchez Moran *et al.* 2001). Among the 45 PMCs surveyed in the wild type, all the meiocytes have 12 bivalents at metaphase I, with a mean of 20.56 ± 1.49 (from 18 to 24) chiasmata per cell (Figure S5A). However, only 1.65 ± 1.03 bivalents with 1.71 ± 1.25 chiasmata per cell were observed among 204 PMCs in *Osmsh4-1* (Figure S5B). We also generated a double mutant between *Osmsh4* and *Osmsh5* and analyzed its chiasma number. The mean chiasma number per cell was 1.76 ± 1.20 (n = 115) in *Osmsh4 Osmsh5* (Figure S4F). Compared with 1.71 ± 1.25 in *Osmsh4-1* and 2.10 ± 0.91 in *Osmsh5* (Luo *et al.* 2013), there was no significant difference detected (t_{317} = 0.45, $P > 0.5$), suggesting OsMSH4 and OsMSH5 probably work in the same pathway (Table 1).

Complete synapsis is achieved in Osmsh4

As one of the most important events in prophase I, successful synapsis necessitates teamwork by numerous genes, otherwise normal synapsis will fail. In *Arabidopsis*, unsynapsed axes are detected in the absence of *AtMSH4* (Higgins *et al.* 2004). In mice, far more severe defects were detected in *msh4*, as homologous chromosomes even failed to align properly (Kneitz *et al.* 2000).

Dual immunodetection was carried out in *Osmsh4-1* meiocytes with antibodies related to either lateral or central elements of SCs to explore the role of OsMSH4 in synapsis. OsREC8, the rice homolog of yeast SCC1/SYN1, is a member of the meiotic cohesion complex. The temporal and spatial distribution of OsREC8 protein covers the whole of prophase I in rice meiosis, making it a perfect marker for monitoring SCs (Shao *et al.* 2011). ZEP1, a transverse filament protein that constitutes the central element of SCs, localizes on chromosomes as punctate foci at leptotene and aligns along the whole length of chromosomes at pachytene when synapsis is complete (Figure S6, A–C). Hundreds of *Osmsh4-1* PMCs were used for dual immunodetection experiments, in which the ZEP1 signals duplicated those in the wild type. Punctate ZEP1 signals were observed at early leptotene (Figure 3A), and these gradually elongated and formed short linear signals from late leptotene to zygotene (Figure 3B).

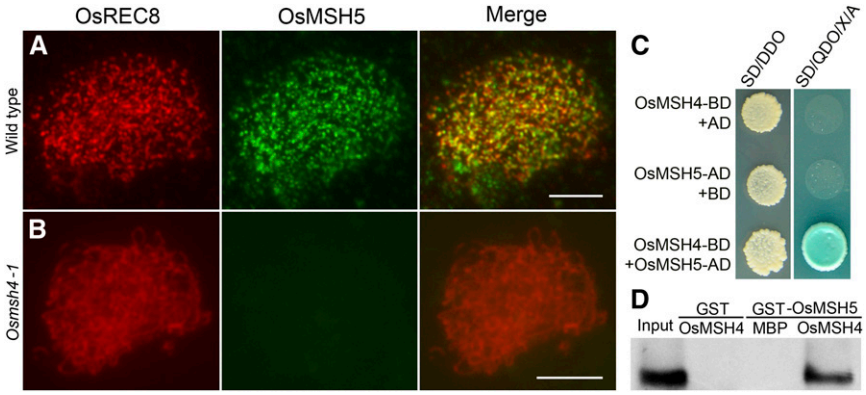

Figure 5 OsMSH4 is essential for the loading of OsMSH5 onto chromosomes. (A) Dual immunolocalization of OsMSH5 in wild type. (B) Dual immunolocalization of OsMSH5 in *Osmsh4-1*. Bars, 5 μm. (C) The interaction between OsMSH4 and OsMSH5 in yeast two-hybrid assays. SD/DDO: SD −Leu −Trp was used to test the cotranformation efficiency. The interaction was tested by the growth of yeast on selection medium SD/QDO/X/A (SD −Ade −His −Leu −Trp +X +A). X: X-α-Gal. A, aureobasidin A; SD medium, minimal, synthetically defined medium for yeast; BD, bait vector; AD, prey vector. (D) The interaction between OsMSH4 and OsMSH5 in GST pull-down assays. Purified GST–OsMSH5 protein was used as positive control (input).The result of MBP–OsMSH4 incubated with GST tag was used as the negative control. Glutathione Sepharose beads coated with GST-OsMSH5 were used to capture either MBP tag or MBP–OsMSH4. The specific affinity of GST–OsMSH5 to MBP–OsMSH4 was shown.

Well-formed continuous linear signals along the whole pachytene chromosomes were also detected (Figure 3C), suggesting that synapsis was fully achieved in *Osmsh4-1*. PAIR2, an axel element of SCs in rice (Nonomura *et al.* 2006), persists on meiotic chromosomes in wild-type PMCs until the end of zygotene (Figure S7A). PAIR3 also works as a meiotic axial element in rice (Wang *et al.* 2011), with a very similar localization pattern to OsREC8 (Figure S7B). We found PAIR2 and PAIR3 both loaded onto chromosomes normally in *Osmsh4-1* meiocytes (Figure 4, A and B).

OsMSH4 acts in conjunction with OsMSH5

It has been shown in other organisms that MSH4 and MSH5 directly interact and drive CO formation as a heterodimer (Bocher *et al.* 1999; Borner *et al.* 2004; Snowden *et al.* 2004; Her *et al.* 2007; Higgins *et al.* 2008). However, no evidence has revealed this direct connection in plants.

We conducted the yeast two-hybrid assay on OsMSH5 and OsMSH4. ORFs of OsMSH5 and OsMSH4 were separately cloned into the related yeast AD vector pGADT7 and the BD vector pGBKT7. These two recombinant vectors were cotransformed into the Y2H Gold yeast strain to trigger their coexpression. We observed bright spots on the double dropout medium, suggesting that the coexpression occurred, and the specific blue-colored spots on the selecting medium represented the positive clones (Figure 5C). Furthermore, we also conducted pull-down assays *in vitro* to confirm this interaction, using GST-fusion proteins and MBP-fusion proteins expressed in *E. coli*. In this assay, GST–OsMSH5, but not GST alone, showed the specific affinity to MBP–OsMSH4 (Figure 5D), further confirming the results from Y2H assays. Thus, the direct interaction between OsMSH4 and OsMSH5 was verified in rice.

The localization of OsMSH5 was investigated in the *Osmsh4-1* mutant. In the PMCs observed, in comparison to the dot-like OsMSH5 signals observed in the wild type (Figure 5A), no OsMSH5 signals were visible on chromosomes of *Osmsh4-1* (Figure 5B), suggesting that the loading of OsMSH5 depends on OsMSH4.

The loading of OsMER3 and OsZIP4 depends on OsMSH4

In rice, the two *zmm* mutants, *Osmer3* and *Oszip4*, show the similar meiotic defects with decreased numbers of chiasmata (Wang *et al.* 2009; Shen *et al.* 2012). To show the relationship of OsMSH4 with OsMER3 and OsZIP4, we performed immunodetection of OsMER3 and OsZIP4 in both wild type and *Osmsh4-1*. In contrast to the dot-like signals observed in the wild type at zygotene (Figure 6, A and B), there was no OsMER3 and OsZIP4 foci in *Osmsh4-1* (Figure 6, C and D), implying that the loading of OsMER3 and OsZIP4 depends on OsMSH4.

The formation of normal HEI10 prominent foci at late pachytene requires OsMSH4

HEI10 is the rice homolog of yeast Zip3 and its loss-of-function mutant showed markedly reduced number of chiasmata as seen in other *zmm* mutants. Immunostaining tests were carried out to investigate its relationship with OsMSH4.

In wild-type meiocytes, HEI10 was first detected at leptotene as punctate foci, and linear signals extended to the entire chromosomes from zygotene to early pachytene (Figure 7A). At late pachytene, some bright foci appeared (Figure 7B), which were proposed to indicate COs (Wang *et al.* 2012).

The immunostaining pattern of HEI10 in *Osmsh4-1* differed from that of OsMER3 and OsZIP4. In *Osmsh4-1*, the loading of HEI10 onto chromosomes was indistinguishable from that of wild type from leptotene to early pachytene when the small dot signals gradually developed into linear signals (Figure 7C). However, at late pachytene, divergence was apparent as the prominent foci did not develop as normal (Figure 7D). We surveyed 20 PMCs from *Osmsh4-1* in late pachytene and found 10.65 ± 2.80 prominent foci in comparison to 24.05 ± 2.17 in wild-type meiocytes ($n = 22$) (Figure 7H). It seems that HEI10 was loaded normally onto chromosomes until early pachytene in *Osmsh4-1*; however, the formation of prominent foci at late pachytene was severely disrupted.

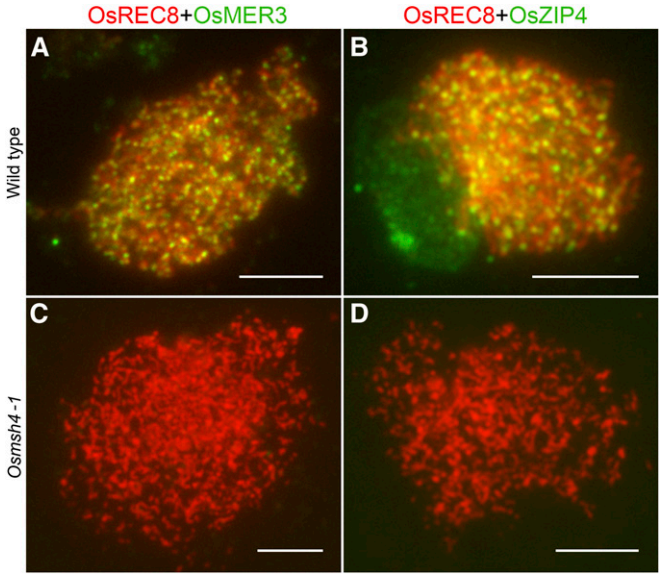

Figure 6 Immunodetection of OsMER3 and OsZIP4 in wild type and *Osmsh4-1*. (A) Staining of OsMER3 at zygotene in the wild type. (B) Staining of OsZIP4 at zygotene in the wild type. (C) Staining of OsMER3 at zygotene in *Osmsh4-1*. (D) Staining of OsZIP4 at zygotene in *Osmsh4-1*. Bars, 5 μm.

In addition, a further yeast two-hybrid assay confirmed the association between OsMSH5 and HEI10. OsMSH5–pGADT7 vector was cotransformed with HEI10–pGBKT7, and their interaction was confirmed by the presence of blue-colored spots on the selecting medium (Figure 7E). In the GST pull-down assays, GST–OsMSH5 could bind to MBP–HEI10 (Figure 7G), providing additional evidence for their direct interaction. However, we did not detect the interaction between OsMSH4 and HEI10 (Figure 7F). Thus, we propose that OsMSH5 may serve as a bridge between OsMSH4 and HEI10.

Discussion

OsMSH4 plays a pivotal role during CO formation

Recombination nodules are large protein complexes that associate with SCs (Stack *et al.* 1993). Early nodules (ENs) and late nodules (LNs) are the two types of recombination nodule involved in SC and CO formation, in which ENs have been presumed to correspond to the initial recombination sites and correlate with the initiation of SC formation (Stack *et al.* 1993), while LNs appear to be associated with COs that are assumed to mature into chiasmata. In budding yeast, Zip3 proteins are regarded as LNs and are considered to mark the final sites of COs (Agarwal and Roeder 2000; Fung *et al.* 2004; Tsubouchi *et al.* 2008). However, Zip3 also interacts with components of ENs, such as Rad51 and Rad57, providing a potential link between ENs and LNs (Agarwal and Roeder 2000). Zip3 presents on meiotic chromosomes as discrete foci and localizes in CO-designated sites (Agarwal and Roeder 2000). However, ZHP-3, the *C. elegans* ortholog of budding yeast Zip3, shows highly dynamic localization (Bhalla *et al.* 2008); RNF212, a protein in mammals with homology to Zip3 and ZHP-3, also dynamically localizes onto chromosomes (Kong *et al.* 2008; Chowdhury *et al.* 2009; Reynolds *et al.* 2013). In rice, HEI10 is the first protein confirmed to mark COs. It also displays dynamic positioning, with dot signals turning to linear signals from leptotene to early pachytene and restricted prominent foci observed from late pachytene to diakinesis (Wang *et al.* 2012). The early staining of HEI10 may represent early recombination, while the restricted foci seen during late pachytene may represent COs.

All ZMM foci are regarded as LNs in budding yeast and are considered to mark the final sites of COs (Agarwal and Roeder 2000; Fung *et al.* 2004; Tsubouchi *et al.* 2008). All MSH4-marked interactions may progress into COs (Lynn *et al.* 2007). However, in mouse and *Arabidopsis*, MSH4 foci occur in substantially greater numbers than the final COs, suggesting that MSH4 may participate in the processing of intermediates that do not generate COs but assist in CO formation (Higgins *et al.* 2004; de Boer *et al.* 2006). In *Arabidopsis*, most MSH4 foci colocalize with RAD51 (Higgins *et al.* 2004), and in mammals MSH4 and RAD51/DMC1 interact directly (Neyton *et al.* 2004), consistent with a direct role of MSH4 in recombination. Notably, in mammals, MSH4 is also found to act in association with the CO-specific markers MLH3 and MLH1 (Santucci-Darmanin *et al.* 2000, 2002; Marcon and Moens 2003), indicating its presence at CO-designated sites and its significance in CO formation.

In *Osmsh4*, HEI10 displayed the same localization pattern with the wild type until early pachytene, indicating the normal processing of early recombination. However, the large bright dots of HEI10 at late pachytene were reduced dramatically compared to wild type. The specific localization pattern of HEI10 suggested a probable defect in the final aggregation onto CO-destined sites, conforming to the working model in which MSH4 forms a heterodimer with MSH5 and plays a role in late recombination processes. The heterodimers bind to the progenitors of dHjs to ensure their stable formation during zygotene to early pachytene and promote the final resolution of dHjs to mature COs at late pachytene, suggesting a role in late recombination (Borner *et al.* 2004; Page and Hawley 2004; Snowden *et al.* 2004). Thus, the absence of either protein will prevent the formation of the heterodimer, which in turn may cause instability of dHj formation and interfere with their development into COs; proteins associated with COs may then be unable to find specific sites to localize to. Since OsMSH5 was unable to localize onto chromosomes in the absence of OsMSH4, the formation of OsMSH4–OsMSH5 heterodimer was completely disrupted. Thus, the sites designated as COs could not form as usual, leading to the disrupted localization pattern of prominent HEI10 foci in *Osmsh4*. In general, OsMSH4 appears to mainly function in late recombination and CO formation but not the early processes, as the SCs were well formed and early localization of HEI10 was not affected in the mutants. Together, these data provided vital clues concerning the partnership between OsMSH5 and

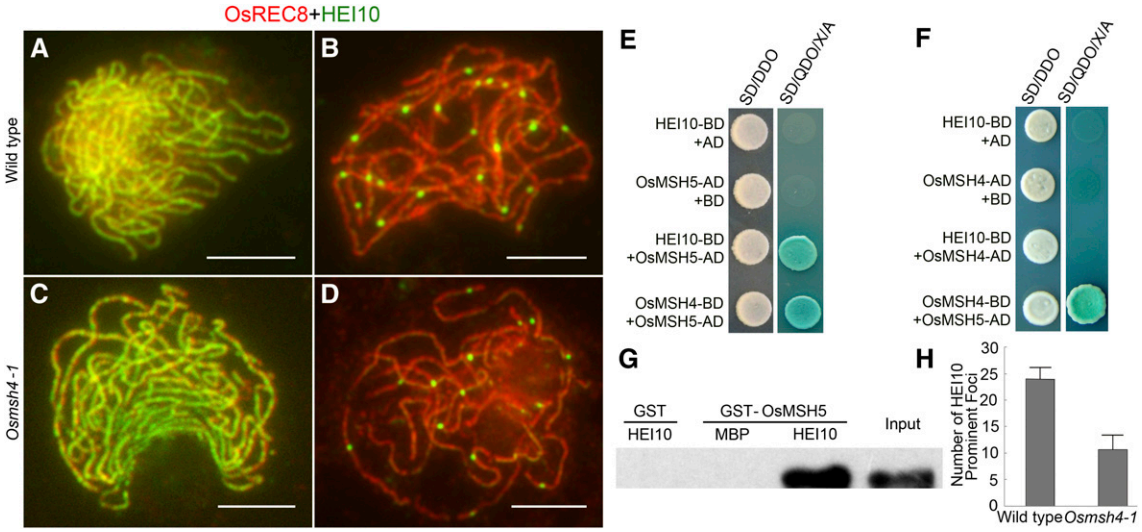

Figure 7 OsMSH4 affects the formation of HEI10 prominent foci. (A and C) Staining for HEI10 at zygotene in wild type and *Osmsh4-1*. (B and D) Staining for HEI10 at late pachytene in wild type and *Osmsh4-1*. Bars, 5 μm. (E) HEI10 interacted with OsMSH5 in yeast two-hybrid assays. The interactions were verified by the growth of yeast on selection medium SD/QDO/X/A. The blue dots from coexpression of OsMSH4 and OsMSH5 were used as positive control. (F) HEI10 did not interact with OsMSH4 in yeast two-hybrid assays. (G) OsMSH5 bound to HEI10 in GST pull-down assays. Purified GST–OsMSH5 protein was used as positive control (input). The result of MBP–HEI10 incubated with GST tag was used as the negative control. Glutathione Sepharose beads coated with GST-OsMSH5 were used to capture either MBP tag or MBP–HEI10. GST–OsMSH5 specifically bound to HEI10. (H) Statistical contrast of HEI10 prominent foci between wild type and *Osmsh4-1*.

OsMSH4 in processing recombination intermediates during the formation of COs.

Except for the results from immunostaining, our studies also revealed a reduction in the chiasma frequency in *Osmsh4*. In *Osmsh4-1*, the chiasma number was reduced to no more than 10% of the wild type. Besides, the number of chiasmata per cell in *Osmsh5* was also decreased to 10% of the wild type (Luo *et al.* 2013). The reduction in *Osmsh4* and *Osmsh5* was much greater than the other *zmm* mutants in rice, such as *Oszip4* and *Osmer3*, which affected the formation of 70–80% of COs, leaving ~30% chiasmata in the mutants (Wang *et al.* 2009, 2012; Shen *et al.* 2012). Considering these results, we suggest that OsMSH4 in association with OsMSH5 plays a far more crucial role in the formation of COs than other ZMM proteins.

The relationship of OsMSH4 with other ZMM proteins

In budding yeast, the ZMM protein groups are involved in many meiotic events. Zip2–4 proteins are implicated in ubiquitinylation and/or SUMOylation processes and are likely to work cooperatively in the modification of protein interactions (Perry *et al.* 2005; Cheng *et al.* 2006). Furthermore, Mer3 and Msh4/Msh5 probably mediate local recombination interactions in the early and late stages, respectively (Hollingsworth *et al.* 1995; Novak *et al.* 2001; Nakagawa and Kolodner 2002). During pachytene, these proteins extensively colocalize, as shown by the colocalization of Zip2–Zip3, Zip4–Zip2, and Zip2–Msh4 (Agarwal and Roeder 2000; Novak *et al.* 2001; Tsubouchi *et al.* 2006). In *Arabidopsis*, *Atmsh4* and *Atmsh5* mutants show great reduction in CO formation and these proteins colocalize with each other in wild-type PMCs (Higgins *et al.* 2008). Moreover, HEI10 in *Arabidopsis* colocalizes with AtMLH1 from pachytene to diakinesis (Chelysheva *et al.* 2012). In rice, colocalization between OsMER3 and early HEI10 signals has also been shown, suggesting their cooperation in processing recombination intermediates in the early stages of meiotic prophase I (Wang *et al.* 2012). In addition to the known classical ZMM genes, other genes with ZMM-related phenotypes have also been discovered in recent years. *PARTING DANCERS* (*PTD*), a novel gene, was found to be epistatic to ZMMs in *Arabidopsis*, and mutation in this gene causes a reduction in COs (Wijeratne *et al.* 2006). Moreover, recent studies have revealed that PTD interacts with SHOC1, the *Arabidopsis* ortholog to Zip2, demonstrating its close relationship with classical ZMM proteins (Macaisne *et al.* 2008, 2011).

OsMSH4 plays a pivotal role in the localization of other ZMM proteins. In *Osmsh4*, chiasma frequency was shown to exhibit a catastrophic reduction, and the localization of OsMER3 and OsZIP4 onto chromosomes was eliminated. These findings led us to propose that OsMSH4 functions upstream of both OsMER3 and OsZIP4. The absence of OsMSH4 also affected the formation of prominent HEI10 foci; in *Osmsh5*, the formation of prominent HEI10 foci was also disrupted (Luo *et al.* 2013), implying that as a heterodimer, the two function in the same way. In the yeast two-hybrid assays and pull-down tests, we showed evidence of multiple interactions among different ZMM proteins. In addition to confirming the OsMSH4–OsMSH5 interaction, we concurrently detected a physical association between OsMSH5 and HEI10. So far, no direct evidence has been

presented concerning the relationships between ZMM proteins in plants, even though there have been many claims that they are functionally related, based solely on their colocalization in cytological experiments. Therefore, these findings may offer great help in drawing the interaction network of ZMM proteins. Furthermore, the interaction between OsMSH5 and HEI10 suggested an indirect interaction between OsMSH4 and HEI10 with OsMSH5 serving as a bridge, providing indirect evidence for the indispensable role of OsMSH4 in the localization of HEI10.

Taken together, our data suggest that OsMSH4 functions in conjunction with OsMSH5 to regulate the formation of the majority of crossovers in rice and these two proteins function upstream of other ZMMs. We can also deduce that the ZMM complex in rice may not only be a functional complex but also a real physical one held together by direct or indirect associations at specific times, if only transiently.

Acknowledgments

This work was supported by grants from the Ministry of Sciences and Technology of China (2012AA10A301 and 2011CB944602), and the National Natural Science Foundation of China (31360260, 31230038, and U1302261).

Literature Cited

Agarwal, S., and G. S. Roeder, 2000 Zip3 provides a link between recombination enzymes and synaptonemal complex proteins. Cell 102: 245–255.

Allers, T., and M. Lichten, 2001 Differential timing and control of noncrossover and crossover recombination during meiosis. Cell 106: 47–57.

Baumann, P., F. E. Benson, and S. C. West, 1996 Human Rad51 protein promotes ATP-dependent homologous pairing and strand transfer reactions in vitro. Cell 87: 757–766.

Bhalla, N., D. J. Wynne, V. Jantsch, and A. F. Dernburg, 2008 ZHP-3 acts at crossovers to couple meiotic recombination with synaptonemal complex disassembly and bivalent formation in *C. elegans*. PLoS Genet. 4: e1000235.

Bocher, T., A. Barusevicius, T. Snowden, D. Rasio, S. Guerrette *et al.*, 1999 hMSH5: a human MutS homologue that forms a novel heterodimer with hMSH4 and is expressed during spermatogenesis. Cancer Res. 59: 816–822.

Borner, G. V., N. Kleckner, and N. Hunter, 2004 Crossover/noncrossover differentiation, synaptonemal complex formation, and regulatory surveillance at the leptotene/zygotene transition of meiosis. Cell 117: 29–45.

Borts, R. H., S. R. Chambers, and M. F. Abdullah, 2000 The many faces of mismatch repair in meiosis. Mutat. Res. 451: 129–150.

Chelysheva, L., D. Vezon, A. Chambon, G. Gendrot, L. Pereira *et al.*, 2012 The *Arabidopsis* HEI10 is a new ZMM protein related to Zip3. PLoS Genet. 8: e1002799.

Chen, C., W. Zhang, L. Timofejeva, Y. Gerardin, and H. Ma, 2005 The *Arabidopsis ROCK-N-ROLLERS* gene encodes a homolog of the yeast ATP-dependent DNA helicase MER3 and is required for normal meiotic crossover formation. Plant J. 43: 321–334.

Cheng, C. H., Y. H. Lo, S. S. Liang, S. C. Ti, F. M. Lin *et al.*, 2006 SUMO modifications control assembly of synaptonemal complex and polycomplex in meiosis of *Saccharomyces cerevisiae*. Genes Dev. 20: 2067–2081.

Chowdhury, R., P. R. Bois, E. Feingold, S. L. Sherman, and V. G. Cheung, 2009 Genetic analysis of variation in human meiotic recombination. PLoS Genet. 5: e1000648.

de Boer, E., P. Stam, A. J. Dietrich, A. Pastink, and C. Heyting, 2006 Two levels of interference in mouse meiotic recombination. Proc. Natl. Acad. Sci. USA 103: 9607–9612.

de Vries, S. S., E. B. Baart, M. Dekker, A. Siezen, D. G. de Rooij *et al.*, 1999 Mouse MutS-like protein Msh5 is required for proper chromosome synapsis in male and female meiosis. Genes Dev. 13: 523–531.

Edelmann, W., P. E. Cohen, B. Kneitz, N. Winand, M. Lia *et al.*, 1999 Mammalian MutS homologue 5 is required for chromosome pairing in meiosis. Nat. Genet. 21: 123–127.

Fung, J. C., B. Rockmill, M. Odell, and G. S. Roeder, 2004 Imposition of crossover interference through the nonrandom distribution of synapsis initiation complexes. Cell 116: 795–802.

Her, C., N. X. Zhao, X. L. Wu, and J. D. Tompkins, 2007 MutS homologues hMSH4 and hMSH5: diverse functional implications in humans. Front. Biosci. 12: 905–911.

Higgins, J. D., S. J. Armstrong, F. C. Franklin, and G. H. Jones, 2004 The *Arabidopsis* MutS homolog AtMSH4 functions at an early step in recombination: evidence for two classes of recombination in *Arabidopsis*. Genes Dev. 18: 2557–2570.

Higgins, J. D., J. Vignard, R. Mercier, A. G. Pugh, F. C. H. Franklin *et al.*, 2008 AtMSH5 partners AtMSH4 in the class I meiotic crossover pathway in *Arabidopsis thaliana*, but is not required for synapsis. Plant J. 55: 28–39.

Hoffmann, E. R., and R. H. Borts, 2004 Meiotic recombination intermediates and mismatch repair proteins. Cytogenet. Genome Res. 107: 232–248.

Hollingsworth, N. M., L. Ponte, and C. Halsey, 1995 MSH5, a novel MutS homolog, facilitates meiotic reciprocal recombination between homologs in *Saccharomyces cerevisiae* but not mismatch repair. Genes Dev. 9: 1728–1739.

Keeney, S., C. N. Giroux, and N. Kleckner, 1997 Meiosis-specific DNA double-strand breaks are catalyzed by Spo11, a member of a widely conserved protein family. Cell 88: 375–384.

Kneitz, B., P. E. Cohen, E. Avdievich, L. Zhu, M. F. Kane *et al.*, 2000 MutS homolog 4 localization to meiotic chromosomes is required for chromosome pairing during meiosis in male and female mice. Genes Dev. 14: 1085–1097.

Kolas, N. K., and P. E. Cohen, 2004 Novel and diverse functions of the DNA mismatch repair family in mammalian meiosis and recombination. Cytogenet. Genome Res. 107: 216–231.

Kong, A., G. Thorleifsson, H. Stefansson, G. Masson, A. Helgason *et al.*, 2008 Sequence variants in the *RNF212* gene associate with genome-wide recombination rate. Science 319: 1398–1401.

Li, W., and H. Ma, 2006 Double-stranded DNA breaks and gene functions in recombination and meiosis. Cell Res. 16: 402–412.

Li, Z., E. I. Golub, R. Gupta, and C. M. Radding, 1997 Recombination activities of HsDmc1 protein, the meiotic human homolog of RecA protein. Proc. Natl. Acad. Sci. USA 94: 11221–11226.

Lipkin, S. M., P. B. Moens, V. Wang, M. Lenzi, D. Shanmugarajah *et al.*, 2002 Meiotic arrest and aneuploidy in MLH3-deficient mice. Nat. Genet. 31: 385–390.

Luo, Q., D. Tang, M. Wang, W. Luo, L. Zhang *et al.*, 2013 The role of OsMSH5 in crossover formation during rice meiosis. Mol. Plant **6:** 729–742.

Luo, Q., Y. Li, Y. Shen, and Z. Cheng, 2014 Ten years of gene discovery for meiotic event control in rice. J. Genet. Genomics 41: 125–137.

Lynn, A., R. Soucek, and G. V. Borner, 2007 ZMM proteins during meiosis: crossover artists at work. Chromosome Res. 15: 591–605.

Macaisne, N., M. Novatchkova, L. Peirera, D. Vezon, S. Jolivet *et al.*, 2008 SHOC1, an XPF endonuclease-related protein, is essential for the formation of class I meiotic crossovers. Curr. Biol. 18: 1432–1437.

Macaisne, N., J. Vignard, and R. Mercier, 2011 SHOC1 and PTD form an XPF-ERCC1-like complex that is required for formation of class I crossovers. J. Cell Sci. 124: 2687–2691.

Marcon, E., and P. Moens, 2003 MLH1p and MLH3p localize to precociously induced chiasmata of okadaic-acid-treated mouse spermatocytes. Genetics 165: 2283–2287.

Mercier, R., D. Vezon, E. Bullier, J. C. Motamayor, A. Sellier *et al.*, 2001 SWITCH1 (SWI1): a novel protein required for the establishment of sister chromatid cohesion and for bivalent formation at meiosis. Genes Dev. 15: 1859–1871.

Nakagawa, T., and R. D. Kolodner, 2002 *Saccharomyces cerevisiae* Mer3 is a DNA helicase involved in meiotic crossing over. Mol. Cell. Biol. 22: 3281–3291.

Nakagawa, T., H. Flores-Rozas, and R. D. Kolodner, 2001 The MER3 helicase involved in meiotic crossing over is stimulated by single-stranded DNA-binding proteins and unwinds DNA in the 3′ to 5′ direction. J. Biol. Chem. 276: 31487–31493.

Neyton, S., F. Lespinasse, P. B. Moens, R. Paul, P. Gaudray *et al.*, 2004 Association between MSH4 (MutS homologue 4) and the DNA strand-exchange RAD51 and DMC1 proteins during mammalian meiosis. Mol. Hum. Reprod. 10: 917–924.

Nonomura, K., M. Nakano, M. Eiguchi, T. Suzuki, and N. Kurata, 2006 PAIR2 is essential for homologous chromosome synapsis in rice meiosis I. J. Cell Sci. 119: 217–225.

Novak, J. E., P. B. Ross-Macdonald, and G. S. Roeder, 2001 The budding yeast Msh4 protein functions in chromosome synapsis and the regulation of crossover distribution. Genetics 158: 1013–1025.

Osman, K., J. D. Higgins, E. Sanchez-Moran, S. J. Armstrong, and F. C. Franklin, 2011 Pathways to meiotic recombination in *Arabidopsis thaliana*. New Phytol. 190: 523–544.

Page, S. L., and R. S. Hawley, 2004 The genetics and molecular biology of the synaptonemal complex. Annu. Rev. Cell Dev. Biol. 20: 525–558.

Perry, J., N. Kleckner, and G. V. Borner, 2005 Bioinformatic analyses implicate the collaborating meiotic crossover/chiasma proteins Zip2, Zip3, and Spo22/Zip4 in ubiquitin labeling. Proc. Natl. Acad. Sci. USA 102: 17594–17599.

Puizina, J., J. Siroky, P. Mokros, D. Schweizer, and K. Riha, 2004 Mre11 deficiency in *Arabidopsis* is associated with chromosomal instability in somatic cells and Spo11-dependent genome fragmentation during meiosis. Plant Cell 16: 1968–1978.

Reynolds, A., H. Qiao, Y. Yang, J. K. Chen, N. Jackson *et al.*, 2013 RNF212 is a dosage-sensitive regulator of crossing-over during mammalian meiosis. Nat. Genet. 45: 269–278.

Ross-Macdonald, P., and G. S. Roeder, 1994 Mutation of a meiosis-specific MutS homolog decreases crossing over but not mismatch correction. Cell 79: 1069–1080.

Sanchez Moran, E., S. J. Armstrong, J. L. Santos, F. C. Franklin, and G. H. Jones, 2001 Chiasma formation in *Arabidopsis thaliana* accession Wassileskija and in two meiotic mutants. Chromosome Res. 9: 121–128.

Santucci-Darmanin, S., D. Walpita, F. Lespinasse, C. Desnuelle, T. Ashley *et al.*, 2000 MSH4 acts in conjunction with MLH1 during mammalian meiosis. FASEB J. 14: 1539–1547.

Santucci-Darmanin, S., S. Neyton, F. Lespinasse, A. Saunieres, P. Gaudray *et al.*, 2002 The DNA mismatch-repair MLH3 protein interacts with MSH4 in meiotic cells, supporting a role for this MutL. homolog in mammalian meiotic recombination. Hum. Mol. Genet. 11: 1697–1706.

Schwacha, A., and N. Kleckner, 1997 Interhomolog bias during meiotic recombination: meiotic functions promote a highly differentiated interhomolog-only pathway. Cell 90: 1123–1135.

Shao, T., D. Tang, K. Wang, M. Wang, L. Che *et al.*, 2011 OsREC8 is essential for chromatid cohesion and metaphase I monopolar orientation in rice meiosis. Plant Physiol. 156: 1386–1396.

Shen, Y., D. Tang, K. Wang, M. Wang, J. Huang *et al.*, 2012 The role of ZIP4 in homologous chromosome synapsis and crossover formation in rice meiosis. J. Cell Sci. 125(Pt 11): 2581–2591.

Snowden, T., S. Acharya, C. Butz, M. Berardini, and R. Fishel, 2004 hMSH4-hMSH5 recognizes Holliday junctions and forms a meiosis-specific sliding clamp that embraces homologous chromosomes. Mol. Cell 15: 437–451.

Stack, S., J. Sherman, L. Anderson, and L. Herickhoff, 1993 Meiotic nodules in vascular plants, pp. 301–311 in *Chromosomes Today*. Springer-Verlag, New York.

Sym, M., and G. S. Roeder, 1994 Crossover interference is abolished in the absence of a synaptonemal complex protein. Cell 79: 283–292.

Tsubouchi, T., H. Zhao, and G. S. Roeder, 2006 The meiosis-specific zip4 protein regulates crossover distribution by promoting synaptonemal complex formation together with zip2. Dev. Cell 10: 809–819.

Tsubouchi, T., A. J. Macqueen, and G. S. Roeder, 2008 Initiation of meiotic chromosome synapsis at centromeres in budding yeast. Genes Dev. 22: 3217–3226.

Wang, K., M. Wang, D. Tang, Y. Shen, B. Qin *et al.*, 2011 PAIR3, an axis-associated protein, is essential for the recruitment of recombination elements onto meiotic chromosomes in rice. Mol. Biol. Cell 22: 12–19.

Wang, K., M. Wang, D. Tang, Y. Shen, C. Miao *et al.*, 2012 The role of rice HEI10 in the formation of meiotic crossovers. PLoS Genet. 8: e1002809.

Wang, K. J., D. Tang, M. Wang, J. F. Lu, H. X. Yu *et al.*, 2009 MER3 is required for normal meiotic crossover formation, but not for presynaptic alignment in rice. J. Cell Sci. 122: 2055–2063.

Wijeratne, A. J., C. Chen, W. Zhang, L. Timofejeva, and H. Ma, 2006 The *Arabidopsis thaliana PARTING DANCERS* gene encoding a novel protein is required for normal meiotic homologous recombination. Mol. Biol. Cell 17: 1331–1343.

Youds, J. L., and S. J. Boulton, 2011 The choice in meiosis: defining the factors that influence crossover or non-crossover formation. J. Cell Sci. 124: 501–513.

Zalevsky, J., A. J. MacQueen, J. B. Duffy, K. J. Kemphues, and A. M. Villeneuve, 1999 Crossing over during *Caenorhabditis elegans* meiosis requires a conserved MutS-based pathway that is partially dispensable in budding yeast. Genetics 153: 1271–1283.

Zickler, D., and N. Kleckner, 1999 Meiotic chromosomes: integrating structure and function. Annu. Rev. Genet. 33: 603–754.

Communicating editor: A. Houben

GENETICS

Supporting Information
http://www.genetics.org/lookup/suppl/doi:10.1534/genetics.114.168732/-/DC1

Crossover Formation During Rice Meiosis Relies on Interaction of OsMSH4 and OsMSH5

Lei Zhang, Ding Tang, Qiong Luo, Xiaojun Chen, Hongjun Wang, Yafei Li, and Zhukuan Cheng

DOI: 10.1534/genetics.114.168732

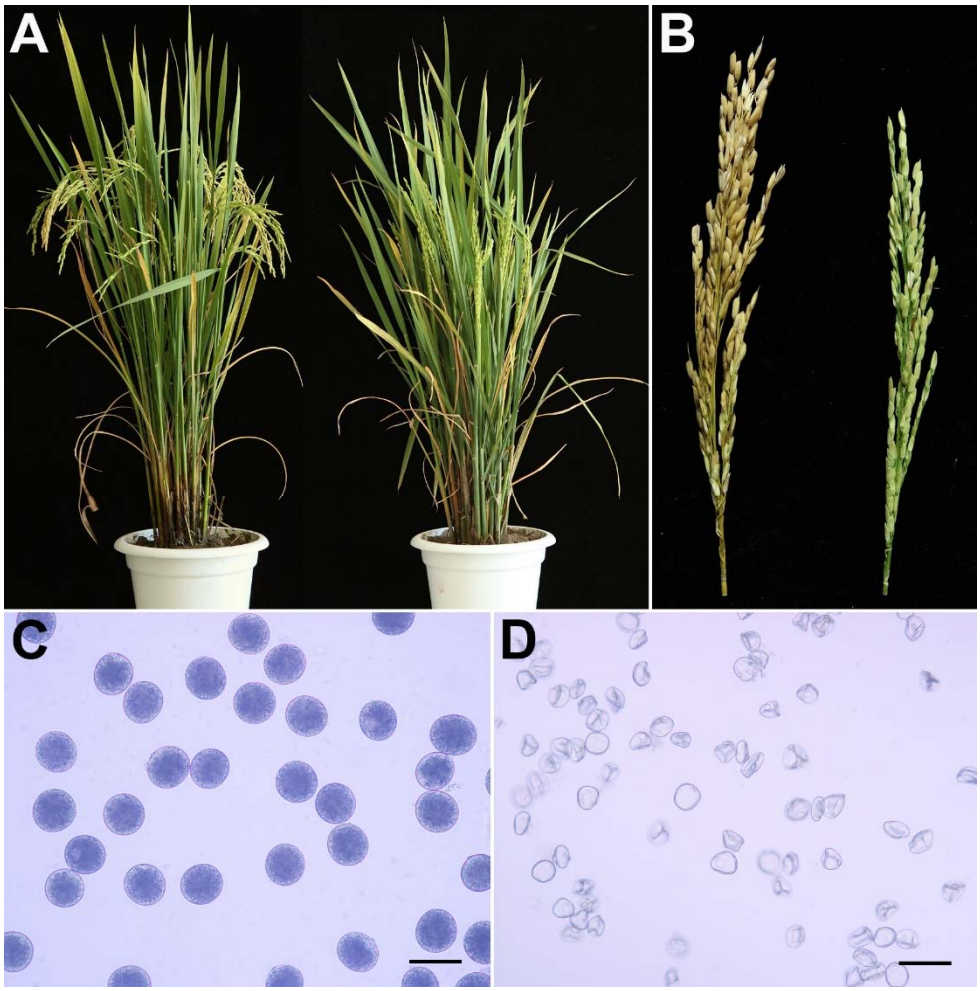

Figure S1 Phenotype characterization of the *Osmsh4-1* mutant.

A, Comparison of a wild type (WT) plant (left) and an *Osmsh4-1* plant (right).

B, Comparison of WT panicles (left) and *Osmsh4-1* panicles (right).

C, I_2-KI staining of wild type pollen grains.

D, I_2-KI staining of *Osmsh4-1* pollen grains. Scale bars, 50 μm.

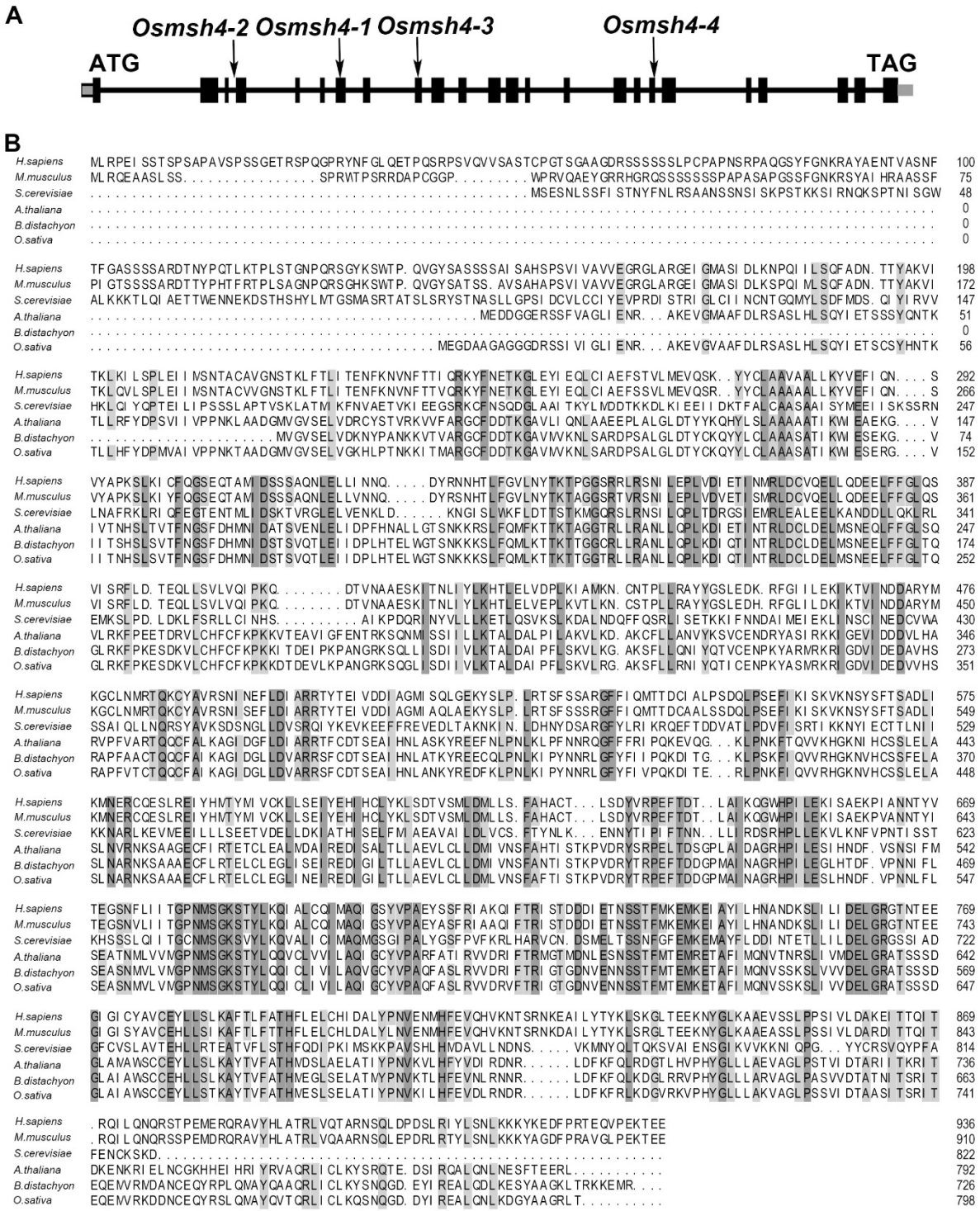

Figure S2 Organization of the *OsMSH4* gene and the protein alignment of MSH4 homologues.

A, Schematic representation of the *OsMSH4* gene and mutation sites in *Osmsh4* alleles. Translated regions are shown as black boxes and untranslated regions are shown as lines. The arrows indicate different mutation sites of *Osmsh4* mutants. B, Protein alignment of MSH4 homologs. Identical amino acids are shaded in gray, while similar amino acids are shaded in silver gray.

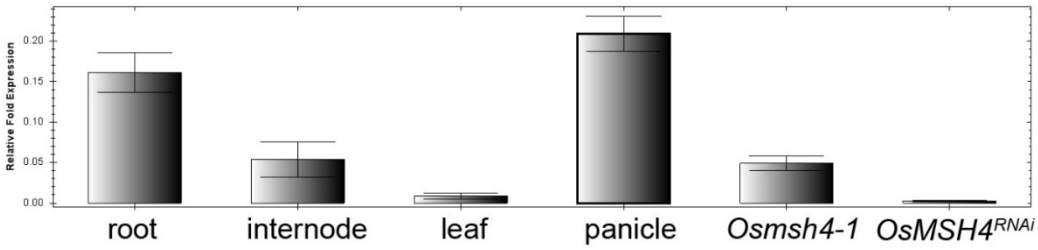

Figure S3 Expression analysis of *OsMSH4*. Transcription levels of *OsMSH4* in both wild type and *Osmsh4* (*Osmsh4-1*, *OsMSH4*^{RNAi}) displayed by Real-Time PCR, with *Ubiquitin* as the endogenous control. Error bars represent SD (n = 3).

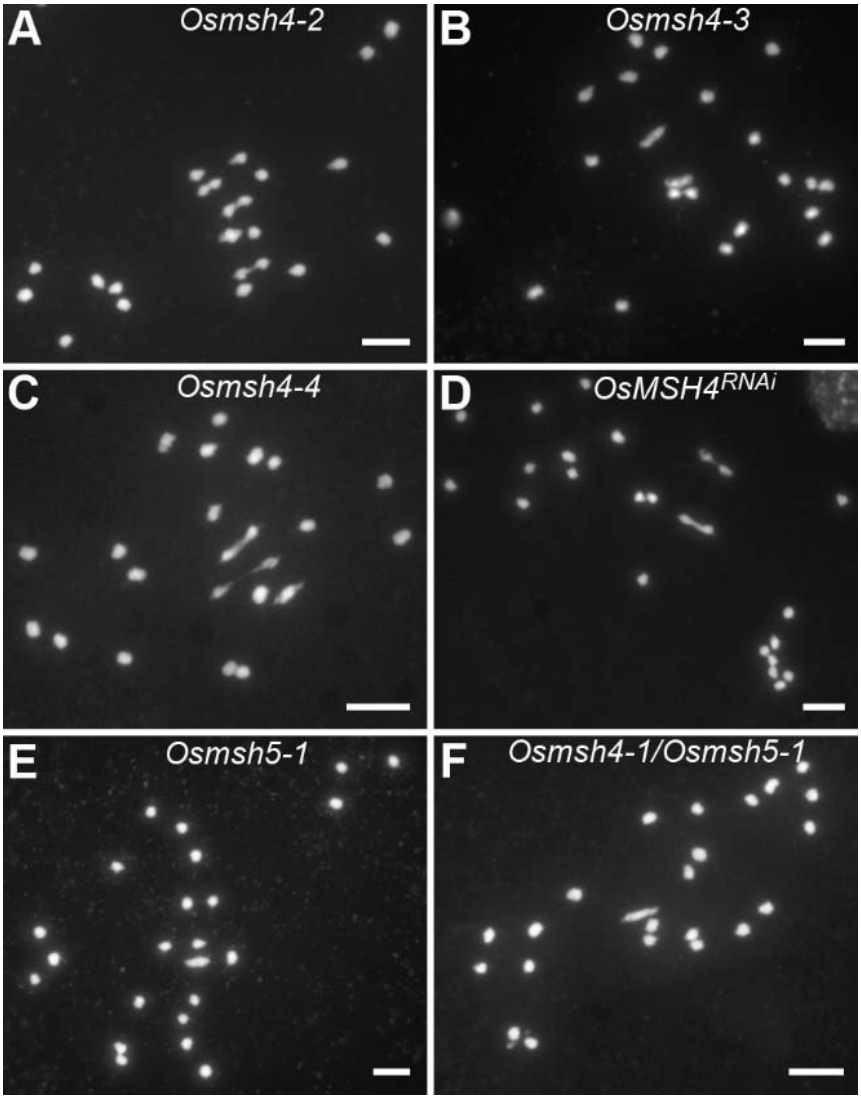

Figure S4 Defects in different mutants.

A, *Osmsh4-2*.

B, *Osmsh4-3*.

C, *Osmsh4-4*.

D, *OsMSH4*^{RNAi}.

E, *Osmsh5-1.*

F, *Osmsh4-1 Osmsh5-1*.

Chromosomes were stained with DAPI. Scale bars, 5 μm.

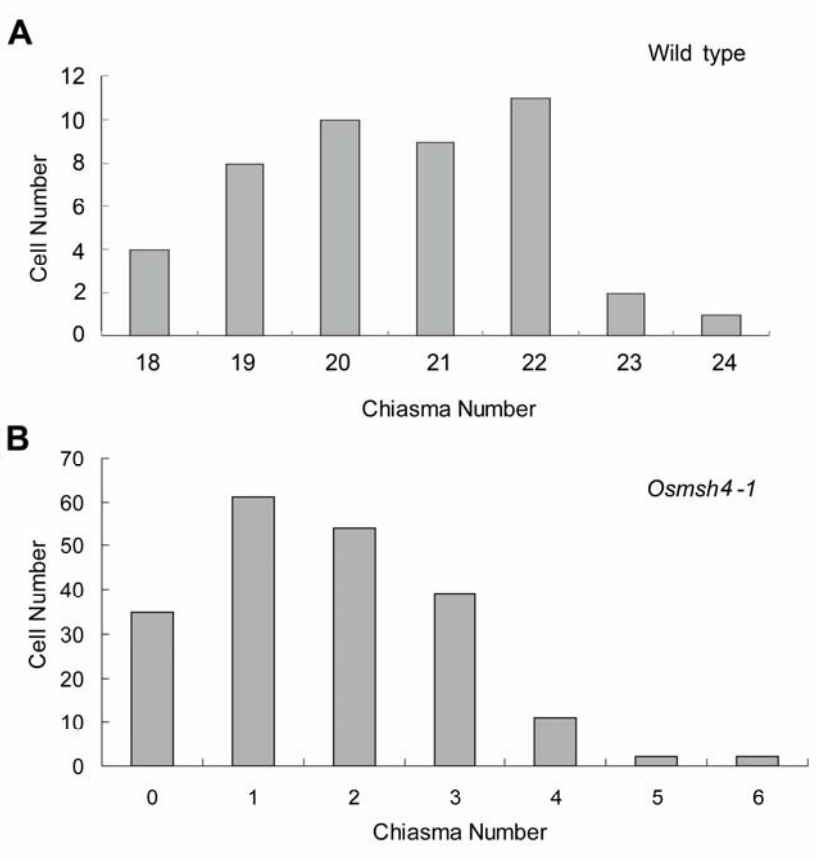

Figure S5 Chiasma distribution in wild type and *Osmsh4-1*.

A, Statistical analysis of the chiasma distribution in wild type meiocytes.

B, Statistical analysis of the chiasma distribution in *Osmsh4-1* meiocytes.

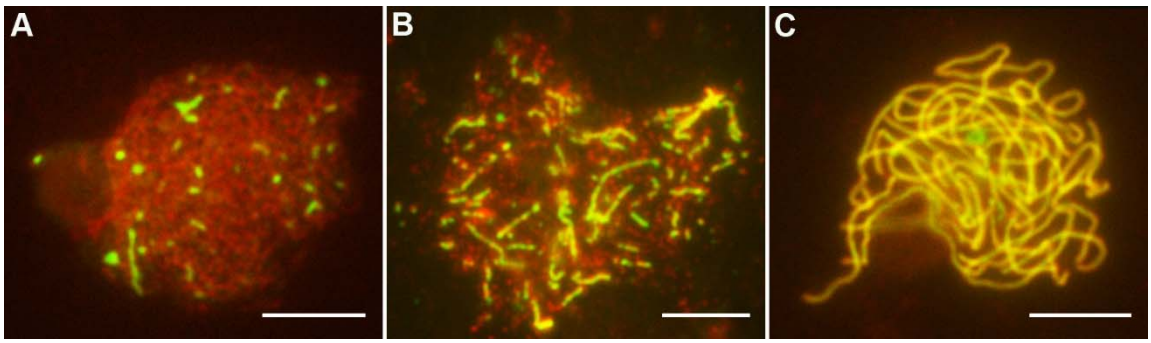

Figure S6 Immunolocalization of OsREC8 (red) and ZEP1 (green) in wild type meiocytes.

A, The localization of ZEP1 at leptotene.

B, The localization of ZEP1 at zygotene.

C, The localization of ZEP1 at pachytene.

OsREC8 signals (red) were used to indicate chromosomes. Scale bars, 5 μm.

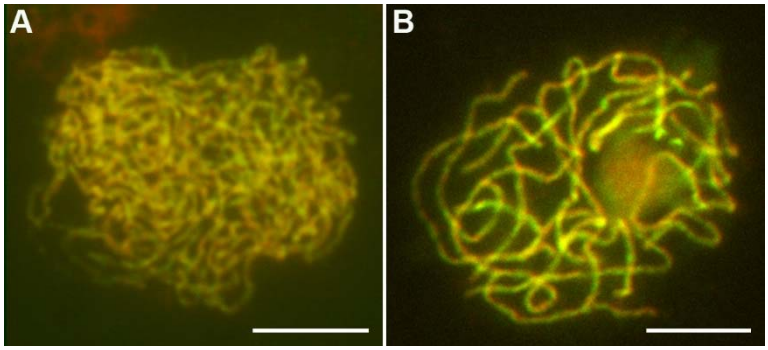

Figure S7 Immunolocalization of OsREC8, PAIR2 and PAIR3 in wild type meiocytes.

A, The localization of PAIR2 (green) at zygotene.

B, The localization of PAIR3 (green) at pachytene.

OsREC8 (red) signals were used to indicate chromosomes. Scale bars, 5 μm.

Table S1 STS primers used in this study

Primer	Forward	Reverse
P1	5′-TGCCCTACACTGGAGAAT-3′	5′-CAGCCACAGTACATAACA-3′
P2	5′-GGCTCGATCTCATTCTATAT-3′	5′-ACGTACCAAATGTAAAGTGT-3′
P3	5′-AGCAGTACTAAAGTTCAGC-3′	5′-GACTTACCAAAGTGGCTCA-3′
P4	5′-AGGTACTGATTCTCATGCTCG-3′	5′-CAACATTGGCACAATCAAGG-3′
P5	5′-CTCCCTCTCGACGACTTGA-3′	5′-TACCAGCAGATTCAGGATT-3′
P6	5′-CCAGCACTACCATAAAACA-3′	5′-CTGGTGCTAGGTAATGATG-3′
P7	5′-AAATATCTGATCCCAGTG-3′	5′-AAATATCTGATCCCAGTG-3′